ISSN 1674-1056
http://cpb.iphy.ac.cn
http://iopscience.iop.org/cpb
中国物理 B
Chinese Physics
中国物理
Chinese Physics B

Current diffusion and efficiency droop in vertical light emitting diodes

R Q Wan(万荣桥), T Li(李滔), Z Q Liu(刘志强), X Y Yi(伊晓燕), J X Wang(王军喜), J H Li(李军辉), W H Zhu(朱文辉), J M Li(李晋闽), L C Wang(汪炼成)

Citation: Chin. Phys. B . 2019, 28(1): 017203. **doi:** 10.1088/1674-1056/28/1/017203

Journal homepage: http://cpb.iphy.ac.cn; http://iopscience.iop.org/cpb

What follows is a list of articles you may be interested in

Recent observations of negative longitudinal magnetoresistance in semimetal

Xi-Tong Xu(许锡童), Shuang Jia(贾爽)

Chin. Phys. B . 2016, 25(11): 117204. **doi:** 10.1088/1674-1056/25/11/117204

Enhanced performances of AlGaInP-based light-emitting diodes with Schottky current blocking layers

Ma Li, Shen Guang-Di, Gao Zhi-Yuan, Xu Chen

Chin. Phys. B . 2015, 24(9): 097202. **doi:** 10.1088/1674-1056/24/9/097202

Current diffusion and efficiency droop in vertical light emitting diodes*

R Q Wan(万荣桥)[1], T Li(李滔)[1], Z Q Liu(刘志强)[2,3], X Y Yi(伊晓燕)[2,3], J X Wang(王军喜)[2,3], J H Li(李军辉)[1], W H Zhu(朱文辉)[1], J M Li(李晋闽)[2], and L C Wang(汪炼成)[1,†]

[1] *State Key Laboratory of High Performance Complex Manufacturing, College of Mechanical and Electrical Engineering, Central South University, Changsha* 410083, *China*

[2] *Semiconductor Lighting Technology Research and Development Center, Institute of Semiconductors, Chinese Academy of Sciences, Beijing* 100083, *China*

[3] *College of Materials Science and Opto-Electronic Technology, University of Chinese Academy of Sciences, Beijing* 101408, *China*

(Received 21 June 2018; revised manuscript received 7 November 2018; published online 30 December 2018)

Current diffusion is an old issue, nevertheless, the relationship between the current diffusion and the efficiency of light emitting diodes (LEDs) needs to be further quantitatively clarified. By incorporating current crowding effect (CCE) into the conventional ABC model, we have theoretically and directly correlated the current diffusion and the internal quantum efficiency (IQE), light extraction efficiency (LEE), and external quantum efficiency (EQE) droop of the lateral LEDs. However, questions still exist for the vertical LEDs (V-LEDs). Here firstly the current diffusion length L_s(I) and L_s(II) have been clarified. Based on this, the influence of CCE on the EQE, IQE, and LEE of V-LEDs were investigated. Specifically to our V-LEDs with moderate series resistivity, L_s(III) was developed by combining L_s(I) and L_s(II), and the CCE effect on the performance of V-LEDs was investigated. The wall-plug efficiency (WPE) of V-LEDs ware investigated finally. Our works provide a deep understanding of the current diffusion status and the correlated efficiency droop in V-LEDs, thus would benefit the V-LEDs' chip design and further efficiency improvement.

Keywords: efficiency droop, vertical light emitting diodes, current crowding effect, current blocking layer

PACS: 72.90.+y **DOI:** 10.1088/1674-1056/28/1/017203

1. Introduction

The current diffusion issue and its related current crowding effect (CCE) are important for the optoelectrical devices, such as laser diode (LD) and light emitting diodes (LEDs).[1–3] The theory of current spreading under a linear stripe top contact geometry has been reported by Thompson.[4] They claimed that the current density is inversely square dependent on the distance from the metal electrode edge.[4] Guo and Schubert[5–7] found in a lateral p-side-up mesa LED, the current exponentially decays from the metal electrode with a characteristic current diffusion length (L_s). For a lateral current-injection scheme, Joyce,[8] Rattier,[9] and Schubert[7] also claimed an exponential decay of the current density over distance. Yet the L_s is related with $J(0)$, current density at the edge of the contact. Some experiments have been set up to evaluate the L_s, such as through the high-resolution mapping of near-field electroluminescence (EL), thermal radiation from optical and infra-red (IR) microscopes,[10,11] specially designed pattern,[12] device, and circuit model.[13] Current diffusion status obviously influences the ultimate efficiency of LEDs. The variation of the lateral carrier's density arising from different current diffusion status obviously correlates with the internal quantum efficiency (IQE). Moreover, as the carriers tend to crowd under the metal electrode, a large percentage of the generated photons will be absorbed by the metal electrode instead of being extracted out. This reduces the light extraction efficiency (LEE). As EQE is related with IQE and LEE, the CCE could significantly affect the IQE, LEE, and thus ultimately the EQE droop level. LEE droop inherited from the CCE has been revealed by Cao,[14] Li,[15] and our group.[16] Various countermeasures have been adopted to increase the L_s to boost the EQE, such as plasma treatment of the p-type GaN region underneath the bonding pad of the electrode,[17] the geometrical parameter optimization,[18–20] special chip design (such as interdigitated multipixel array (IMPA) chip design,[21] interdigitated mesa geometry design,[22]) by incorporating transparent conductive layer (TCL),[23,26] tunnel junction,[27,28] or current blocking layer (CBL).[29,30]

However, there is still a lack of direct and theoretical correlation linking CCE and EQE droop in these reports, and to date there are no reports to single out the relevant contribution of CCE to IQE, LEE, and ultimate EQE droop. The original ABC model,[31] which is widely adopted to explain the effi-

*Project supported by the National Key Research and Development Program of China (Grant No. 2018YFB0406702), the Professorship Start-up Funding (Grant No. 217056), the Innovation-Driven Project of Central South University, China (Grant No. 2018CX001), the Project of State Key Laboratory of High-Performance Complex Manufacturing, Central South University, China (Grant No. ZZYJKT2018-01), and Guangzhou Science & Technology Project of Guangdong Province, China (Grant Nos. 201704030106 and 2016201604030035).

†Corresponding author. E-mail: liancheng_wang@csu.edu.cn, wanglc@semi.ac.cn

© 2019 Chinese Physical Society and IOP Publishing Ltd

ciency droop, does not take into account the CCE due to the variation of current distribution (carrier density) versus position. The variation of LEE as function of the injected current is also not available in this model. Therefore, the average IQE, LEE, and EQE have to be adopted to account for the variation of current distribution in the real devices. By incorporating the CCE into the conventional ABC model, we have theoretically correlated the relationship between the CCE and the IQE, LEE and EQE droop for conventional lateral LEDs.[32] We can accurately and vividly examine the influence of specific current diffusion parameters to the ultimate IQE, LEE, and EQE. Schemes including CBL, TCL, and series resistance (R_s) engineering for addressing the CCE, have also been investigated with this approach.

2. Results and discussion

2.1. Current diffusion model for V-LEDs

Generally, the current would flow vertically across the diode junction, or laterally to area away from the electrode area, with the resistance to be named vertical resistance (R_v) and lateral resistance (R_l), respectively. R_v consists of n-GaN and p-GaN bulk resistances (R_n, R_p), metal contact resistance (R_c), and junction resistance (R_d). R_d dynamically varies with the current injection magnitude with $R_d = \partial V/\partial I$ from the typical diode I–V characteristics. Instead of vertical resistance, we adopted vertical resistivity ρ_v with unit of $\Omega\cdot\text{cm}^2$, whereas the unit of resistance is Ω. For the lateral current path, the conventionally adopted transparent current electrodes (TCEs) (i.e., ITO, Ni/Au) on p-GaN and n-GaN act as the major current diffusion layer, whose lateral resistance represents the lateral resistance R_l for LED device.

A general formula for L_s has also been derived,[32] to be the ratio of the vertical resistivity (ρ_v, $\Omega\cdot\text{cm}^2$) to the lateral resistance (R_l, Ω),

$$L_s = \sqrt{\frac{\rho_v}{R_l}}. \tag{1}$$

The V-LEDs chip and its equivalent circuit model is shown in Figs. 1(a) and 1(b), respectively. The vertical resistivity ρ_v ($\Omega\cdot\text{cm}^2$) in V-LEDs includes: metal/p-GaN contact resistivity $\rho_{c,p}$, p-GaN bulk resistivity $\rho_p t_p$, junction resistivity R_J, n-GaN bulk resistivity $\rho_n t_n$, and metal/n-GaN contact resistivity $\rho_{c,n}$. $\rho_n t_n$ and $\rho_{c,n}$ are comparatively small and thus can be neglected. R_l is dominated by $R_{l,n}$. For typical V-LEDs, n-GaN functions as the current spreading layer, so $R_l = \rho_n/t_n$. ρ_v is uncertain, and different L_s are adopted by different groups[7,14,33]

$$L_s(\text{I}) = \sqrt{\frac{\rho_c + \rho_p t_p}{\rho_n/t_n}} \text{ or } L_s(\text{II}) = \sqrt{\frac{n_{\text{ideal}} kT/J(0)e}{\rho_n/t_n}}, \tag{2}$$

where ρ_c is the metal/p-GaN contact resistivity, ρ_n and ρ_p are the n-GaN and p-GaN resistivity, and t_n and t_p are the thickness of n-GaN and p-GaN. n_{ideal} is the diode ideality factor.

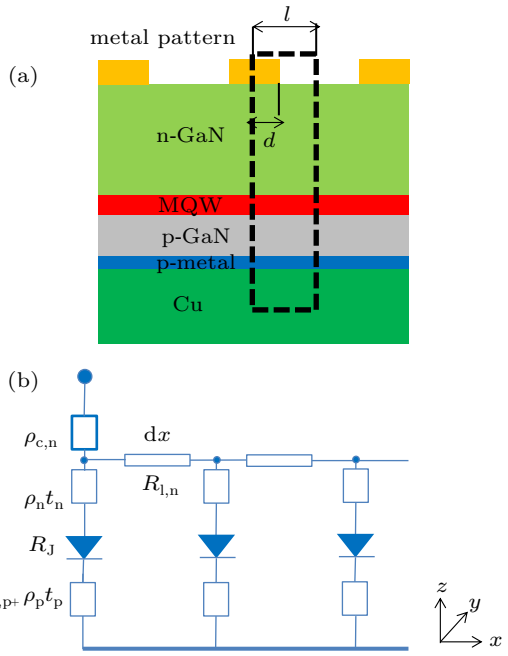


Fig. 1. (a) V-LEDs chip structure cross section and (b) the equivalent circuit model corresponding to the unit cell circled in panel (a).

The circuit in Fig. 1(b) shows several nodes separated by a distance dx. Assuming that $V(x)$ is the voltage in the n-GaN along the x-direction, then $V(x)$ is the voltage drop across the n-GaN resistance of length dx. Calculating the difference in voltage drop between two adjacent resistors and applying Kirchhoff's current law to the node located between the two resistors yield the differential equation and the current diffusion length equation can be simplified into the following two cases. We omit the detail derivation process which can be referred to Schubert's book.[7]

i) When

$$(\rho_{c,p} + \rho_p t_p) \gg \frac{(n_{\text{ideal}} kT/e)}{J(x)}, \quad L_s(\text{I}) = \sqrt{\frac{(\rho_c + \rho_p t_p)}{\rho_n/t_n}}. \tag{3}$$

ii) When

$$(\rho_{c,p} + \rho_p t_p) \ll \frac{(n_{\text{ideal}} kT/e)}{J(x)},$$

$$L_s(\text{II}) = \sqrt{\frac{t_n n_{\text{ideal}} kT}{\rho_n Je}} = \sqrt{\frac{n_{\text{ideal}} kT/J(0)e}{\rho_n/t_n}}. \tag{4}$$

Note that $J(0)$ is the current at the edge of the metal contact. It is revealed from the derivation process that: whether choose L_s(I) or L_s(II) in V-LEDs is determined by the relative magnitude of the bulk resistivity $\rho_{c,p} + \rho_p t_p$ and the junction resistivity $(n_{\text{ideal}} kT/e)/J(x)$. Equally speaking, for V-LEDs with relatively higher operation voltage ($\rho_{c,p} + \rho_p t_p$ dominates in ρ_v during operation), L_s(I) dominates over L_s(II); for V-LEDs with a much lower operation voltage

$((n_{\text{ideal}}kT/e)/(J(x))$ dominates), L_s(II) should be adopted instead. Note that the value of L_s(I) is a constant and L_s(II) is dynamically varied in terms of J.

Since the influence of CCE on V-LEDs for case II has been investigated in Ref. [29], here we concentrate on case I and compare the results obtained between case I and II. The calculation model is similar to that described in Ref. [29], by incorporating the current diffusion length L_s(I) and L_s(II) into the widely used ABC model. L_s(II) is simplified to be

$$L_s(\text{II}) = \sqrt{\frac{k_v}{J(0)}}, \tag{5}$$

where

$$k_v = \frac{tn_{\text{ideal}}kT}{\rho e}. \tag{6}$$

Take our typical V-LED with size of 1×1 mm as a reference, the spacing between the neighboring electrodes is around 200 μm. Hence, we choose L_s(I) = 24.5, 50, 100, and 200 μm, which are equal to L_s(II) with $k_v = 6 \times 10^{-4}$, 2.5×10^{-3}, 1×10^{-2}, 4×10^{-2} at $J(0) = 100$ A/cm^2, respectively. L_s(I) = 200 μm suggests that the current well diffused status and L_s(I) = 24.5 μm suggests the poor current diffused status.

2.2. Influence of CCE on V-LEDs' efficiency based on L_s(I): a fixed current diffusion length

For V-LED, due to much larger thermal conductivity of Cu ($\sim$400 W·m^{-1}·°C^{-1}) compared with that of sapphire ($\sim$40 W·m^{-1}·°C^{-1}),[38] the thermal effect is not considered in our model. Figure 2(a) shows the lateral carrier's distribution $n(x)$ under various L_s (24.5, 50, 100, and 200 μm) and J (10, 100 A/cm^2). $n(x)$ remains to be constant under the shadow area (the metal contact area) and decays out of the shadow area. When L_s is fixed, $n(x)$ line curves are parallel with each other at different J. A higher J certainly leads to a larger $n(x)$. A larger L_s causes the $n(x)$ curve to decay slowly. Figure 2(b) shows the position dependant IQE, i.e., IQE(x) curves. Refer to the ABC model (Eq. (S1)), we know that IQE(x) reaches its maximum when $n(x) = n'(x) = \sqrt{A/C} = 5.5 \times 10^{18}$ cm^{-3}. So when $n(x)$ approaches $n(x) = 5.5 \times 10^{18}$ cm^{-3}, IQE(x) increases, and vice versa. From the $n(x)$ curves in Fig. 2(a), we know that in all the diffusion status, $n(x)$ is larger than $n'(x)$, and decreases when x increases. Thus, IQE(x) monotonically increases. IQE(x) for $J = 10$ A/cm^2 is undoubtedly larger than IQE(x) for $J = 100$ A/cm^2 due to higher $n(x)$ at larger J. The average EQE can be obtained by integrating the IQE(x), LEE(x), and $n(x)$ (Eq. (S7)), the average IQE can be obtained by integrating the IQE(x) and $n(x)$ (Eq. (S8)). Figure 2(c) shows the EQE-I(J) curves. Some trends can be clearly observed: i) all the EQE-I(J) curves show typical droop characteristics, which is caused by the superimposed effects of CCE and other effects; ii) both of EQE-I$_{\text{peak}}$ and droop length L_d increase with L_s. The droop length is defined as the current range between the current density for the peak EQE$_{\text{peak}}$ and that for the EQE$_{\text{peak}}$/e; iii) EQE saturates at larger L_s. For example, at $J = 60$ A/cm^2, EQE-I= 0.34 for $L_s = 100$ is close to EQE-I= 0.35 for $L_s = 200$ μm. Figure 2(d) shows the IQE-I(J) curves. IQE-I also increases and IQE-I(J) droop relieves with an increased L_s, which is quite similar to that of EQE-I. The difference between the EQE-I(J) and IQE-I(J) curves is that IQE-I$_{\text{peak}}$ keeps almost invariant, whereas EQE-I$_{\text{peak}}$ increases obviously with L_s. This indicates that the LEE-I effect cannot be neglected and it plays a role in determining the average EQE-I. Figure 2(e) demonstrates average LEE-I(J) in terms of different L_s. At fixed L_s, the LEE-I first increases

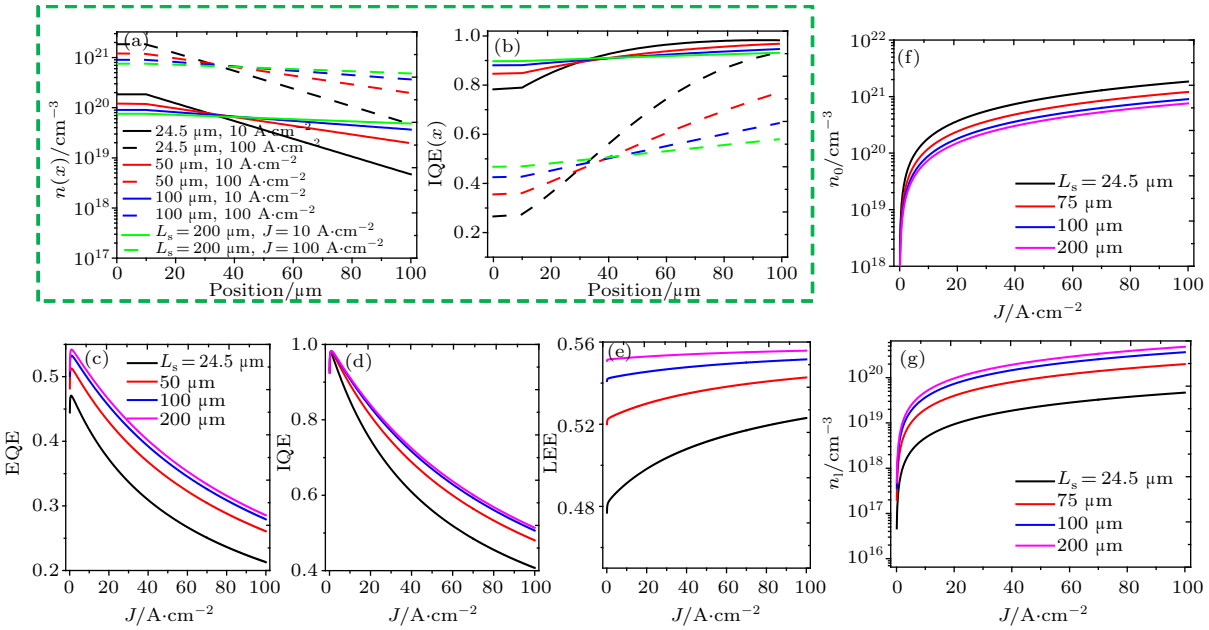


Fig. 2. (a) Lateral carrier's distribution $n(x) - I$; (b) the corresponding IQE(x) curves under various L_s (24.5, 100, and 200 μm) and J (10, 100 A/cm^2); (c) the average EQE-I(J); (d) the average IQE-I(J); (e) the average LEE-I(J) curves; (f) $n_0 - I$; and (g) $n_l - I(J)$ curves for case I.

rapidly at relatively small J region and then slowly increase when J further increases. At a fixed J (e.g., 40 A/cm^2), the average LEE-I also firstly increases rapidly at a lower L_s value (increases from LEE-I= 0.50 for $L_s = 24.5$ μm to LEE-I= 0.534 for $L_s = 50$ μm), and then almost saturates at larger L_s value (LEE = 0.547 and 0.553 for $L_s = 100$ and 200 μm, respectively). If L_s is large enough, for example at $L_s = 1000$ μm, LEE-I should reach its limit of LEE-$I_{max} = (0.1 \times d + 0.6 \times 9d)/10d = 0.56$. Figures 2(f) and 2(g) show the concentration of n_0-I and n_1-I as a function of J for different L_s. At fixed L_s, both n_0-I and n_1-I increase monotonically with J. n_1-I increases rapidly at the small J region and slowly increases at larger J region, which resembles the trend of LEE-I(J) in Fig. 2(e). At fixed J, n_0-I decreases and n_1-I increases when L_s increases. n_1-I becomes closest to n_0-I when L_s is large enough at $L_s = 200$ μm, indicating that the carriers are distributed almost uniformly.

All these phenomenon can be easily understood in terms of CCE: at fixed J (fixed total injected carriers within unit time), an increased L_s indicates that more carriers are diffused out of the shadow area, resulting in decreased n_0-I, increased $n_1 - I$, and thus improved LEE$-I$; an improved uniform distribution of carriers leads to improved IQE$-I$; the unambiguous improved IQE$-I$ and LEE$-I$ lead to an ultimately improved EQE$-I$.

2.3. Compare the influence of CCE on V-LEDs' efficiency based on L_s(I) and L_s(II)

We next compare the influence of CCE on V-LEDs' efficiency based on L_s(I) and L_s(II). Figure 3(a) shows the carrier distribution for case I and II at $J = 10$ A/cm^2 and $J = 100$ A/cm^2. At a comparable carrier diffusion level, $n(x)$-II (e.g., $k_v = 6 \times 10^{-4}$) is higher than $n(x)$-I (e.g., L_s(I) = 24.5 μm) outside the shadow region at $J = 10$ A/cm^2. Oppositely, $n(x)$-II (e.g., $k_v = 6 \times 10^{-4}$) is lower than $n(x)$-I (e.g., L_s(I) = 24.5 μm) outside the shadow region at large $J = 100$ A/cm^2. This is due to the inherent characteristics of L_s(I) and L_s(II): L_s(I) keeps constant whereas L_s(II) is extremely large (small) at low (high) J. With the increase of current diffusion capability, e.g., L_s(I) = 100 μm and $k_v = 1 \times 10^{-2}$ for L_s(II), $n(x)$-I and $n(x)$-II curves are almost overlapped. Figure 3(b) shows the corresponding IQE(x) curves for case I and II at $J = 10$ A/cm^2 and $J = 100$ A/cm^2. Similarly, IQE(x) increases when $n(x)$ approaches $n'(x)$. From $n(x)$ distribution in Fig. 3(a), at low L_s, i.e., L_s(I) = 24.5 μm and $k_v = 6 \times 10^{-4}$, it is easy to understand that the IQE(x) curve shows a more parabola characteristics. For $k_v = 6 \times 10^{-4}$ and $J = 100$ A/cm^2, the carriers are severely crowded near the shadow area and $n(x)$ approaches $n'(x)$ in the area far from the shadow. Therefore the IQE(x) is quite low under and near the shadow area and high in the area far from the shadow (the green dashed line in Fig. 3(b)). This is reasonable as the L_s is extremely low in this situation (L_s (II) $= \sqrt{k_v/J(0)} < \sqrt{k_v/J}$). Note that this asymmetric distribution of IQE(x) and $n(x)$ leads to a low average IQE, LEE, and thus EQE. Figures 3(c), 3(d), and 3(e) plot the IQE(J), LEE(J), and EQE(J) curves, respectively. It can be observed that there is an intersection between EQE(J) curves of these two cases, with the trend becoming more obvious when k_v or L_s is small (e.g., $L_s = 24.5$ μm and $k_v = 6 \times 10^{-4}$) and disappears when k_v or L_s grow larger (e.g., $L_s = 100$ μm and $k_v = 1 \times 10^{-2}$). When $L_s = 24.5$ μm or $k_v = 6 \times 10^{-4}$, EQE-I_{peak} is much lower (= 0.47) than EQE-II_{peak} (= 0.54), and EQE-I is higher (= 0.21) than EQE-II (= 0.14) when J reaches 100 A/cm^2. EQE-I(J) droop length L_d (over 100 A/cm^2 for $L_s = 24.5$ μm) is obviously larger than that of EQE-II (J) (= 70 A/cm^2 for $k_v = 6 \times 10^{-4}$). IQE(J) curves show similar intersection characteristics, as shown in Fig. 3(c). LEE(J) curves in Fig. 3(d) show that LEE-I rapidly increases initially and then slowly increases with the increase of J, while LEE-II exhibits almost the opposite trend: rapidly

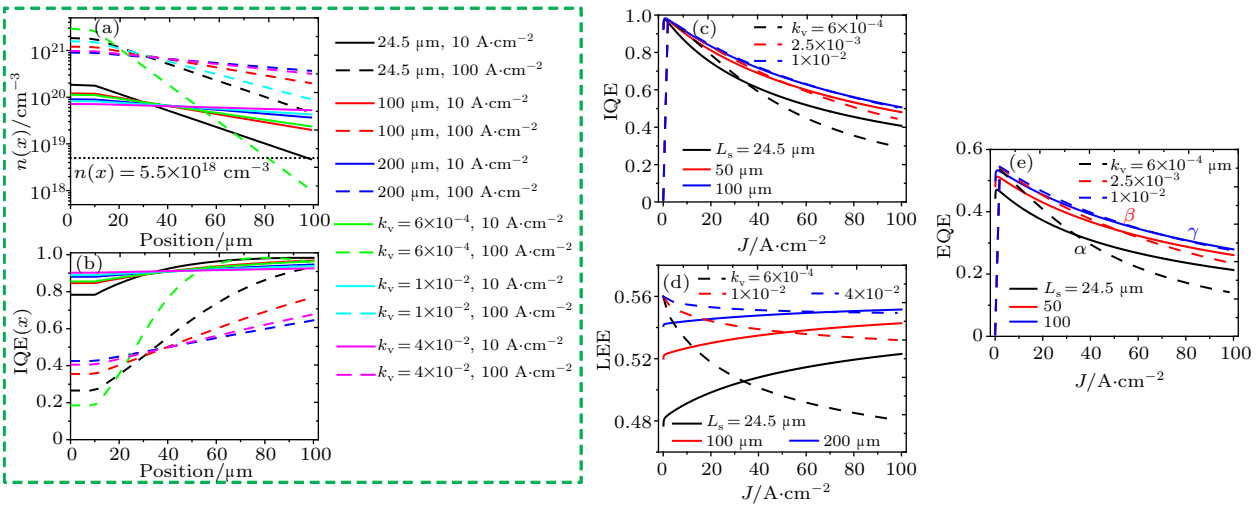


Fig. 3. (a) $n(x)$, (b) IQE(x), (c) IQE(J), (d) LEE(J), (e) EQE(J) curves under various diffusion status and current density. The continuous and dashed lines represent case I and II, respectively.

decreases initially and then slowly decreases. The reasons have been discussed above and in Ref. [29]. This tells us that the opposite variation trend of LEE is the notable reason accounting for the EQE(J) discrepancy between case I and II. At the intersection points (α, β, γ, as shown in Fig. 3(e)), L_s(I) is equal to L_s(II). For example, at intersection point α (33.3 A/cm^2, 0.33), L_s(I) = 24.5 μm = L_s(II) = $\sqrt{6\times10^{-4}/J(0)}$, where $J(0)$ is set to be 100 A/cm^2. This means when $k_v = 6\times10^{-4}$, to reach the shadow edge current $J(0) = 100$ A/cm^2, the inject current is as low as J_α = 33.3 A/cm^2 for case II. This indicates that the current is severely crowded. When k_v increases to 2.5×10^{-3} and 1×10^{-2}, the corresponding J_β and J_γ are 50 A/cm^2 and 100 A/cm^2, respectively. Similarly, this means that, in order to reach $J(0) = 100$ A/cm^2, the inject current should be 50 A/cm^2 and 100 A/cm^2 at $k_v = 1\times10^{-2}$ and 4×10^{-2}, respectively. $J_\gamma = 100$ A/cm^2 means that the current is sufficiently diffused. This comparison gives a more qualitative understanding of the CCE effect on the final efficiency based on diffusion case I and II.

We further listed the EQE, IQE, and LEE values with certain J and L_s (k_v) values in Table 1 to single out the major contributing components accounting for EQE droop for case I and II. Here $k_v = 6\times10^{-4}$, 1×10^{-2}, and L_s = 24.5, 100 μm were chosen for case I and II, corresponding to carrier "crowded" ($k_v = 6\times10^{-4}$, L_s = 24.5 μm) and "diffused" ($k_v = 1\times10^{-2}$, L_s = 100 μm) status, respectively. It can be observed from Table 1 that, at low J = 10 A/cm^2, the increment 7% for IQE-I and 10% for LEE-I together contribute to the ultimate EQE-I enhancement when L_s is increased from 24.5 μm to 100 μm. However, at J = 100 A/cm^2, IQE-I enhancement takes the major responsibility for the EQE enhancement, i.e., IQE is increased by about 24.4% and LEE is increased by only 6% while L_s is increased from 24.5 μm to 100 μm. For fixed L_s, we found IQE-I decrease while LEE-I increases both at the "crowded" state and at the "diffused" state. As listed in Table 1, IQE-I decrease to 48.2% (56%) and LEE-I increases to 106% (101.5%) of the original values when J increases from 10 A/cm^2 to 100 A/cm^2 at L_s = 24.5 μm (100 μm), respectively. The increased LEE-I counteracts the degradation of IQE-I, which is different from case II. In case II, LEE-II decreases to 90.5% ($k_v = 6\times10^{-4}$) and 99.3% ($k_v = 1\times10^{-2}$) when J increases from 10 A/cm^2 to 100 A/cm^2. Nonetheless, we can conclude that for a real chip (fixed k_v or L_s), the EQE droop is mainly ascribed to the degradation of IQE, instead of LEE, for both case I and II.

Table 1. Specific EQE, IQE, and LEE under certain J and k_v for case I and II.

	Case I: L_s = 24.5 μm		L_s = 100 μm		Increment/%		Case II: $k_v = 6\times10^{-4}$		$k_v = 1\times10^{-2}$		Increment/%	
	IQE	LEE	IQE	LEE	IQE	LEE	IQE	LEE	IQE	LEE	IQE	LEE
J = 10 A/cm^2	0.85	0.49	0.91	0.54	7%	10%	0.89	0.53	0.91	0.554	2%	4.5%
J = 100 A/cm^2	0.41	0.52	0.51	0.55	24.4%	6%	0.30	0.48	0.51	0.55	70%	14.6%
γ_1%	48.2%	106%	56%	101%			33.7%	90.5%	56%	99.3%		

2.4. CBL scheme for V-LEDs

For the CBL scheme, the carrier concentration under the shadow could be set to zero ideally. The CBL effects on EQE, IQE, and LEE for case I are shown in Figs. 4(a), 4(b), and 4(c), respectively. EQE-I$_{peak}$ (= 0.586, 0.588, 0.589 for L_s = 24.5, 50, 100 μm, respectively) is increased and almost saturated with CBL design compared with that of non-CBL design (= 0.47, 0.51, 0.53). L_d for EQE-I(J) is actually decreased. While the corresponding L_d is over 100 μm for non-CBL scheme. We found that IQE is actually decreased after incorporating CBL, as shown in Fig. 4(b). For example, IQE= 0.52 decreases to be 0.49 in CBL scheme when L_s = 24.5 μm and J = 60 A/cm^2. Ideally, LEE-I for CBL is kept constant to be 0.6 for the CBL case, higher than the non-CBL case, as shown in Fig. 3(d). We can see that for the CBL scheme, it is the improvement of the LEE, instead of the IQE, that contributes to the ultimate improvement of EQE. The n_0-I and n_1-I were also monotonically increased due to the fact that the carriers are push into the unshadow region by CBL, as shown in Fig. 4(d) and 4(e). Compared with the CBL scheme for case II (Fig. 5 in Ref. [29]), some obvious distinctions can be observed. We also plotted IQE-II curves with and without CBL in Fig. 4(f). As shown in Fig. 4(a), it can be observed that both IQE-I and IQE-II decrease with CBL incorporation. This is due to the increased carrier concentration in the area out of the shadow by the CBL. EQE-II shows intersection characteristics, i.e., it is increased at low J and decreased at large J. EQE-I is unambiguously increased with CBL. Both L_d for EQE-I and EQE-II are decreased. LEE-II is 0.6 for both cases, higher than that of the non-CBL scheme. The enhancement of LEE, instead of IQE, is the root reason and motivation for incorporating CBL for both cases. The difference is that LEE-I increases while LEE-II decreases with J for the non-CBL scheme (Fig. 4(c), and Fig. 2(c) in Ref. [29]). The distinctions of CBL effect on V-LEDs for case I and II result from different features of the defined L_s : L_s(I) is kept constant while L_s(II) is decreased with CBL scheme at fixed k_v. The decreased L_s(II) is attributed to the increase of $J(0)$ (or n_0), as can be seen from Fig. 4(d) and the formula of L_s(II). This indicates that the CBL approach is not effective for case II, but can be very effective for case I.

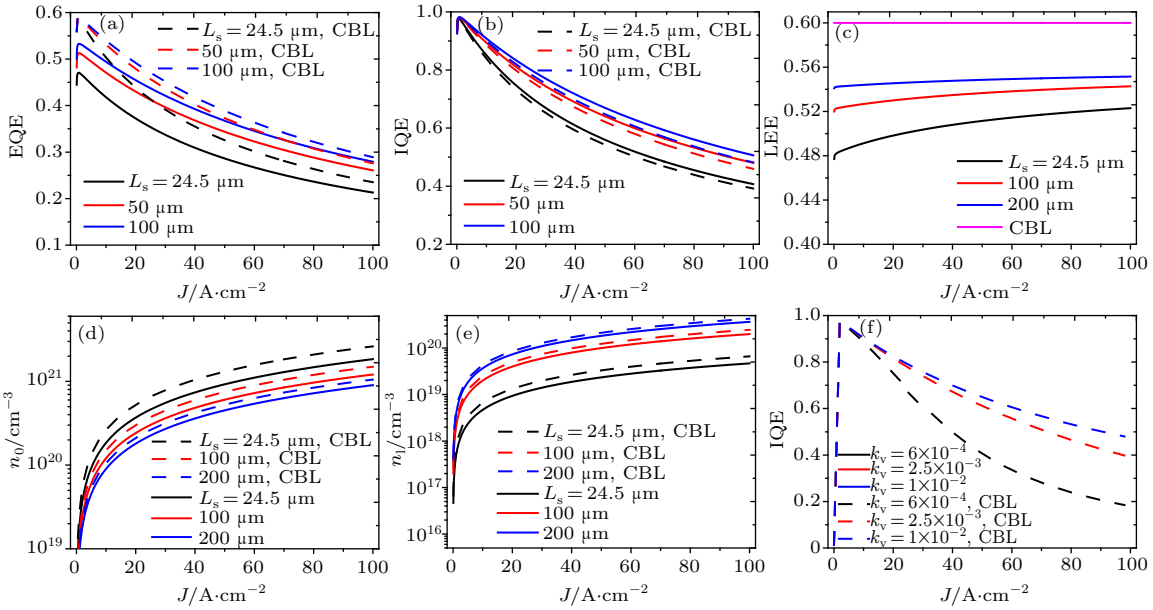


Fig. 4. (a) EQE(J), (b) IQE(J), (c) LEE(J), (d) $n_0(J)$, and (e) $n_1(J)$ curves for non-CBL (continuous line) and CBL (dashed line) for case I; (f) IQE(J) curve for non-CBL (continuous line) and CBL (dashed line) for case II.

2.5. A short summary: influence of CCE for V-LEDs

A short summary can be made here regarding the influence of CCE on EQE, IQE, LEE of V-LEDs: all EQE(J), IQE(J) show typical droop characteristics; EQE-I is lower than EQE-II before the intersection point, yet higher than EQE-II after the intersection point, thus EQE-I(J) curve has a larger L_d; IQE(J) trend is similar to EQE, except that IQE-I and IQE-II have comparable peak values; both LEE increases with an improved current spreading (larger k_v or L_s), yet LEE-I decreases and LEE-II increases with J; both n_0 increases monotonically with increased J, and decreases with an improved current spreading (larger k_v or L_s); both n_1 increases monotonically with an increased k_v or L_s; n_1-I increases monotonically at all current spreading level, while at low k_v status, n_1-II increases first at low J region and then decreases when J further increases (Figs. 2(e) and 2(f) in Ref. [29]); CBL incorporation can improve both LEE, which is the root reason and motivation for both cases. IQE-I and IQE-II will be decreased for both cases.

2.6. Analysis of current diffusion and efficiency droop and wall-plug efficiency (WPE) in our typical V-LEDs device

Now we are to figure out the current diffusion status in our typical V-LEDs device. From above analysis, we know that L_s(II) and L_s(I) actually corresponds to high and low resistive V-LEDs, respectively. However, note that the discussion in Section 2 is actually theoretical prediction for a device when L_s(I) and L_s(II) is adopted. It should be clarified that for real devices, L_s is dynamically varied and actually is the sum of L_s(I) and L_s(II). Refer to Fig. 3(e), when L_s(I) = 24.5 μm and $k_v = 6\times10^{-4}$, L_s(II) is dominate over L_s(I) at J lower than J_α and vice versa, L_s(I) is dominate over L_s(II) at J larger than J_α. Hence, L_s in the real device actually is the sum of L_s(I) and L_s(II). Specifically to our real V-LEDs chips, $\rho_{c,p}+\rho_p t_p = 3.7\times10^{-3}$ Ω·cm^2 and $\rho_p t_p = 1.25\times10^{-4}$ Ω·cm^2, according to the I–V and CTLM (circular transmission line method) test results.[34,35] For nitride-based devices, n_{ideal} actually is abnormally high,[36] to be 2–10. We chose a moderate $n_{ideal} = 5$, then the dynamical junction resistivity $\dfrac{n_{ideal}kT/e}{J(x)}$ is comparable to the constant bulk resistivity $\rho_{c,p}+\rho_p t_p$. For example, when $k_v = 4\times10^{-2}$, at $J = 100$ A/cm^2, it is reasonable to assume $J(0) \sim 100$ A/cm^2, as current is sufficiently diffused. Hence, we have

$$\frac{n_{ideal}kT/e}{J(0)} \approx \frac{5\times0.026\ \text{V}}{100\ \text{A}\cdot\text{cm}^{-2}} = 1.3\times10^{-3}\ \Omega\cdot\text{cm}^2. \quad (7)$$

Both the bulk resistivity and the junction resistivity of the V-LEDs should be incorporated. Refer to L_s(I) and L_s(II) formulas, this should yield a L_s to be the ratio of the total ρ_v to the total R_1. Therefore,

$$L_s(\text{III}) = \sqrt{\frac{\rho_c+\rho_p t_p}{\rho_n/t_n} + \frac{n_{ideal}kT/J(0)e}{\rho_n/t_n}} = \sqrt{k_v\delta + \frac{k_v}{J(0)}}, \quad (8)$$

where $k_v = \dfrac{t_n n_{ideal}kT}{\rho_n\cdot e}$, $\delta = \dfrac{e(\rho_p t_p+\rho_c)}{n_{ideal}kT}$, and δ is calculated to be 2.85×10^{-2} A^{-1}·cm^2 here.

Assuming the sheet resistance ρ_n/t_n of the TCL (usually ITO) is 80 Ω/□, the k_v is calculated to be $\sim 1.6\times10^{-3}$. By using the L_s(III), we can get the EQE-III(J), IQE-III(J), and LEE-III(J) curves in Figs. 5(a)–5(c). We can see that all EQE-III(J) share similar characteristics with EQE-I(J) and EQE-II(J): typical droop trend; the EQE-III(J) droop relieves and L_d increases as the k_v increases. IQE-III shows the droop

characteristics in the similar manner, except that IQE-III$_{peak}$ keeps almost invariant. EQE-III and IQE-III saturates with a finite $k_v = 1\times10^{-2}$ since both L_s(I) (L_s(I) $=\sqrt{k_v\delta}\approx 170$ μm) and L_s(II) (L_s(II) $=\sqrt{\frac{k_v}{J(0)}}\approx 100$ μm) contribute to the total L_s ($=270$ μm). The finite bulk resistivity $\rho_{c,p}+\rho_p t_p$ also helps to boost the L_s(II) as the $J(0)$ is reduced. Combining cases I and II, LEE-III shows obvious trend. With the increase of J, LEE-III first decreases and then increases. We also investigate the EQE(J) results with varied δ. As shown in Fig. 5(d), when k_v is low, e.g., $k_v = 6\times10^{-4}$, EQE(J) increases significantly when δ increases, with EQE(J) = 0.256, 0.32, and 0.35 when $\delta = 2.85\times10^{-3}$, 2.85×10^{-2}, 2.85×10^{-1} A^{-1}·cm^2, respectively at $J = 60$ A/cm^2. Instead, when k_v is high, e.g., $k_v = 1\times10^{-2}$, EQE(J) tends to be more saturated, with EQE(J) = 0.33, 0.35, and 0.36 at $\delta = 2.85\times10^{-3}$, 2.85×10^{-2}, 2.85×10^{-1} A^{-1}·cm^2, respectively, when $J = 60$ A/cm^2. The EQE(J) enhancement is brought by the increased k_v or δ, equally speaking, reduced lateral resistance ($R_{l,n}=\frac{\rho_n}{t_n}$) or increased bulk resistivity ($\rho_v=\rho_p t_p+\rho_c$). Hence, the physics scenario for current diffusion in V-LEDs is simple: ρ_v acts as "current blocker" and $R_{l,n}$ relates with lateral spreading capability. If ρ_v is comparatively extremely low that current would straight flow vertically under the shadow (case II) area and vice versa (case I). For our typical V-LEDs device without TCL or CBL (Fig. 1(b)), L_s is calculated to be ~ 79 μm ($L_s\approx\sqrt{\frac{R_J+\rho_{c,p}}{\rho_n/t_n}}=79$ μm), smaller that the metal finger spacer length l (~ 100 μm). L_s can be increased by increasing ρ_v (e.g., by using high resistive and even Schottky contact metal to p-GaN), decreasing the lateral resistance,[32] or adding more current flow channels (equally speaking, to incorporate TCL). The various laterally flow channels work parallelly to enhance the L_s. For example, we can derivate the L_s in V-LEDs with TCL adopted. For adoption of conventional ITO (~ 40 Ω/□) onto n-GaN, L_s is estimated to be 302 μm,

$$\begin{aligned} L_s &= L_s(\mathrm{ITO})+L_s(n)\\ &=\sqrt{\frac{R_J+\rho_{c,p}}{\rho_{ITO}/t_{ITO}}}+\sqrt{\frac{R_J+\rho_{c,p}}{\rho_n/t_n}}\\ &=223\ \mu\mathrm{m}+79\ \mu\mathrm{m}=302\ \mu\mathrm{m}. \end{aligned} \tag{9}$$

Our approach here provides a feasible and convenient way for L_s derivation.

Now let us proceed to discuss on Wall-plug efficiency (WPE). For all the three cases, high resistive (case I), low resistive (case II), and moderate resistive (case III) V-LEDs, L_s and thus EQE always increases monotonically with ρ_v or k_v according to Eqs. (3), (5), and (8), providing that the high ρ_v-induced heat (case I and III) has a negligible effect. However, this cannot be applied to the WPE. For case II, WPE increases monotonically with k_v, as the ρ_v and thus the dissipated heat power can be neglected due to its inherent extremely low resistance. However, for case I and III, at fixed k_v (or R_l), both W_{op} (the optical power output) and the $W_{consumed}$ (the total consumed electrical power) increase with ρ_v. This cannot guarantee a monotonical increase of WPE $= W_{op}/W_{consumed}$. Hence, an optimized ρ_v should exist to maximize WPE $= W_{op}/W_{consumed}$. We have discussed this for case I in Ref. [29]. The total power consumed can be divided into two parts: voltage drop across the inherent potential (~ 2.6 eV) and heat generated by the R_s. Hence, the WPE can be specifically expressed as follows:

$$\begin{aligned} \mathrm{WPE} &= \frac{W_{photon}}{W_{consumed}}\\ &=\frac{hw\int_0^l \mathrm{IQE}(x)\mathrm{LEE}(x)n(x)\,\mathrm{d}x\hbar\omega}{\frac{Jlhw}{qv}\hbar\omega+(Jlw)^2\frac{R_s}{lw}\frac{h}{v}}\\ &=\frac{\int_0^l \mathrm{IQE}(x)\mathrm{LEE}(x)n(x)\,\mathrm{d}x\hbar\omega}{\frac{Jl}{qv}\hbar\omega+\frac{J^2lR_s}{v}}, \end{aligned} \tag{10}$$

where $\hbar\omega$ is equal to be 2.6 eV, and R_s is the total vertical resistance. By integrating Eqs. S2, S3, 8, S5, S6, and 11, we plot the WPE(δ) curves for case III in Fig. 5(e) at $J = 35$ A/cm^2 and Fig. 5(f) at $J = 100$ A/cm^2, respectively. We purposely chose these J values since for the typical operation currents for the 1 mm square sized V-LEDs chip are 350 mA and 1000 mA. We mark δ_{max} as the value when WPE reaches its maximum and $\delta=\frac{e\rho_v}{n_{ideal}kT}\approx\frac{\rho_v}{0.13}$. L_s is defined as

$$L_s=\sqrt{\frac{n_{ideal}kT\delta}{eR_l}+\frac{n_{ideal}kT}{eJ(0)R_l}}=\sqrt{\frac{0.13\delta+0.13/J(0)}{R_l}}, \tag{11}$$

which is based on L_s(III). At $J = 35$ A/cm^2 (100 A/cm^2), $\delta_{max} = 1.17\times10^{-2}$ (1.15×10^{-2}), 1.50×10^{-2} (1.4×10^{-2}), 2.8×10^{-2} (2.15×10^{-2}), and 5.08×10^{-2} (3.56×10^{-2}) when the lateral resistance $R_l = 80$, 100, 200, and 500 Ω/□. δ_{max} exists for each R_l indicates that no matter how small R_l is, δ is not the lower, the larger in terms of WPE. When J is fixed, the increased δ_{max} with an increased R_l lies in that L_s needs to be boosted for compensating the L_s loss brought by the increase of R_l, to enhance W_{op}. When R_l is fixed, we found δ_{max} almost decreases at the higher J. For example, $\delta_{max} = 2.15\times10^{-2}$ for $R_l = 200$ Ω/□, $J = 100$ A/cm^2 is lower than $\delta_{max} = 2.8\times10^{-2}$ for $R_l = 100$ Ω/□, $J = 35$ A/cm^2. This is due to $W_{consumed}$ increases much faster than W_{op} when J increases. This analysis here provides a rational design guide for V-LEDs working at different rating current. For example, in our V-LEDs device[34] (without ITO), there is only n-GaN to act as the current spreading layer, with its R_l being ~ 80 Ω/□. According to the calculated results in Fig. 5(f), maximum WPE can be achieved at $\delta = 1.4\times10^{-2}$(100 A/cm^2), which corresponds to $\rho_v = \rho_{c,p}+\rho_p t_p = 1.82\times10^{-3}$ Ω·cm^2. Actually, the experimentally obtained ρ_v value for our V-LEDs device

is 3.7×10^{-3} Ω·cm^2, which is close to the ideal ρ_v value. To further reduce the ρ_v can ensure the maximum W_{op} and low forward voltage (V_F) can be achieved simultaneously. However, this will reduce the EQE. Our experimental results also verified the feasibility of our discussion above.[34]

We have carried out many experiments on current diffusion and transparent conductive electrodes in VLEDs. InGaN-based vertical structure light emitting diodes (VLEDs) with multi-layer graphene transparent electrodes with higher optical output have been fabricated and tested, whereas the increased optical output is attributed to the boost diffusion of current by the graphene and also the "block" effect on the vertical direction due to larger contact resistivity between graphene and u-GaN also contributes to this.[24] This is consistent with the theoretical estimation in this article. We used high reflective membrane current blocking layer (CBL) combined with graphene transparent electrodes in V-LEDs, which shows 60% increase in light output power and relieved EQE droop compared with regular V-LEDs.[37] All these results verified the theoretical evaluation and analysis in this article and also valuation and analysis in this article.

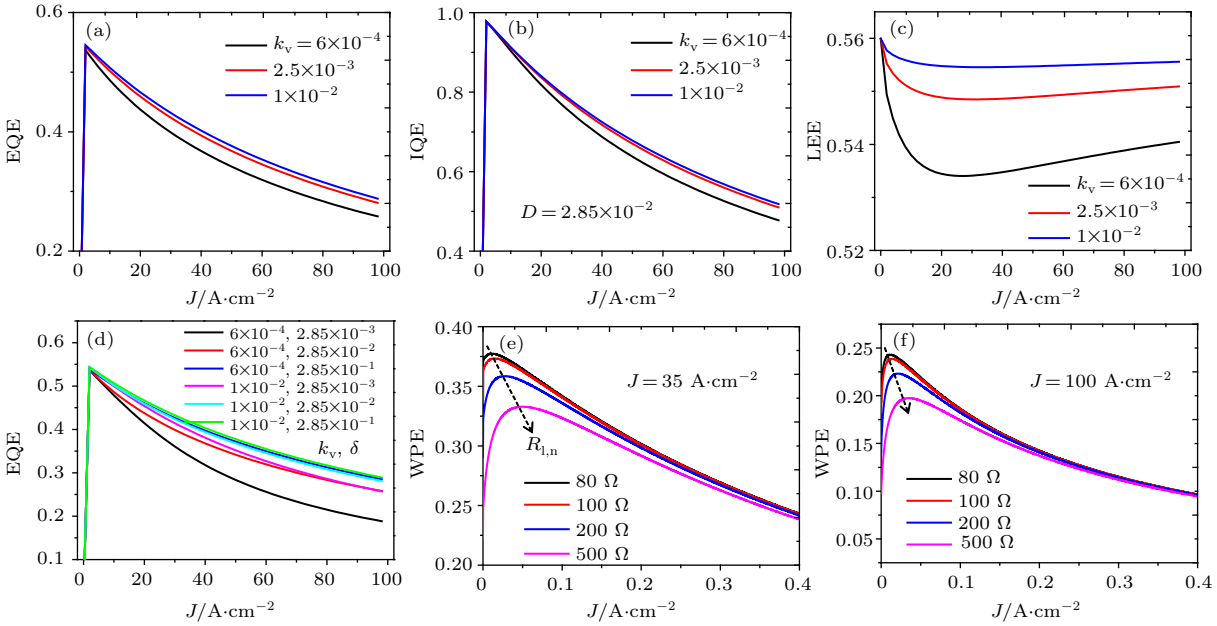


Fig. 5. (a) EQE-III(J), (b) IQE-III(J) and (c) LEE-III(J) curves for case III, moderate resistive V-LEDs; (d) EQE-III(J) curves with varied δ and k_v for case III; WPE(δ) curves for case III at (e) $J = 35$ A/cm^2 and (f) 100 A/cm^2.

3. Conclusion

We have further resolved the questions concerning the current diffusion status in V-LEDs. First, we have derived the formula for L_s(I) and L_s(II), and found that L_s(I) and L_s(II) is fit to relatively more resistive and low resistive V-LEDs, respectively. For V-LEDs with quite low operation voltage, CBL can be effective. Although the IQE decreases with CBL incorporation, it can improve the LEE, contributing to the ultimate improvement of EQE; for V-LEDs with higher operation voltage, the EQE droop is mainly ascribed to the poor LEE, a more conductive current spreading layer is more effective. The influence of CCE based on L_s(I) and L_s(II) to EQE, IQE, LEE of V-LEDs were then comparatively investigated in detail and summarized. Specifically to our V-LEDs, we developed L_s(III) by combining L_s(I) and L_s(II). The CCE effect based on L_s(III) on performance of V-LEDs were investigated then. As to WPE, we found WPE is monotonically increased with an increased k_v for case II and an optimized ρ_v exists for maximum WPE. Our findings should provide a deep and comprehensive understanding of the current diffusion status and efficiency droop in V-LEDs, could benefit the V-LEDs design on current diffusion and thus its further performance enhancement.

References

[1] Zhao Y K, Li Y F, Huang Y P, Wang H, Su X L, Ding W and Yun F 2015 *Chin. Phys. B* **24** 056806

[2] Zhuo X J, Zhang J, Li D W, Yi H X, Ren Z W, Tong J H, Wang X F, Chen X, Zhao B J, Wang W L and Li S T 2014 *Chin. Phys. B* **23** 068502

[3] Yang B, Guo Z Y, Xie N, Zhang P J, Li J, Li F Z, Lin H, Zheng H and Cai J X 2014 *Chin. Phys. B* **23** 048502

[4] Thompson G H B 1980 *Physics of Semiconductor Laser Devices* (New York: John Wiley and Sons)

[5] Guo X and Schubert E 2001 *J. Appl. Phys.* **90** 4191

[6] Guo X and Schubert E 2001 *Appl. Phys. Lett.* **78** 3337

[7] Schubert E F, Gessmann T and Kim J K 2005 *Light Emitting Diodes* (New York: John Wiley and Sons)

[8] Joyce W 1970 *J. Appl. Phys.* **41** 3818

[9] Rattier M, Benisty H, Stanley R, Carlin J, Houdre R, Oesterle U, Smith C, Weisbuch C and Krauss T 2002 *IEEE J. Select. Top. Quantum Electron.* **8** 238

[10] Chernyakov A, Bulashevich K, Karpov S and Zakgeim A 2013 *Phys. Status Solidi A* **210** 466

[11] Calciati M, Goano M, Bertazzi F, Vallone M, Zhou X, Ghione G, Meneghini M, Meneghesso G, Zanoni E, Bellotti E, Verzellesi G, Zhu D and Humphreys C 2014 *AIP Adv.* **4** 067118
[12] Huang S, Fan B, Chen Z, Zheng Z, Luo H, Wu Z, Wang G and Jiang H 2013 *J. Display Technol.* **9** 266
[13] Ebong A, Arthur S, Downey E, Cao X, LeBoeuf S and Merfeld D 2003 *Solid-State Electron.* **47** 1817
[14] Cao B, Li S, Hu R, Zhou S, Sun Y, Gan Z and Liu S 2013 *Opt. Express* **21** 25381
[15] Li C and Wu Y 2012 *IEEE Trans. Electron. Devices* **59** 400
[16] Zhang Y, Zheng H, Guo E, Cheng Y, Ma J, Wang L, Liu Z, Yi X, Wang G and Li J 2013 *J. Appl. Phys.* **113** 014502
[17] Lee H, Pan K, Lin C, Chang Y, Kao F and Lee C 2007 *J. Vac. Sci. Technol. B* **25** 1280
[18] Kim H, Lee J, Huh C, Kim S, Kim D, Park S and Hwang H 2000 *Appl. Phys. Lett.* **77** 1903
[19] Kim H, Park S, Hwang H and Park N 2002 *Appl. Phys. Lett.* **81** 1326
[20] Kim H, Park S J and Hwang H 2001 *IEEE Trans. Electron. Dev.* **48** 1065
[21] Bogdanov M, Bulashevich K, Evstratov I, Zhmakin A and Karpov S 2008 *Semicond. Sci. Technol.* **23** 125023
[22] Guo X, Li Y and Schubert E 2001 *Appl. Phys. Lett.* **79** 1936
[23] Wang L, Liu W, Zhang Y, Zhang Z, Tan S, Yi X, Wang G, Sun X, Zhu H and Demir H 2015 *Nano Energy* **12** 419
[24] Wang L, Zhang Y, Li X, Liu Z, Guo E, Yi X, Wang J, Zhu H and Wang G 2012 *Appl. Phys. Lett.* **101** 061102
[25] Zhang Y, Wei T, Xiong Z, Chen Y, Zhen A, Shan L, Zhao Y, Hu Q, Li J and Wang J 2014 *J. Appl. Phys.* **116** 194301
[26] Zhang Y, Li J, Wei T, Liu J, Yi X, Wang G and Yi F 2012 *Jpn. J. Appl. Phys.* **51** 020204
[27] Jeon S, Song Y, Jang H, Yang G, Hwang S and Son S 2001 *Appl. Phys. Lett.* **78** 3265
[28] Zhang Z, Tan S, Kyaw Z, Ji Y, Liu W, Ju Z, Hasanov N, Sun X and Demir H 2013 *Appl. Phys. Lett.* **102** 193508
[29] Huh C, Lee J, Kim D and Park S 2002 *J. Appl. Phys.* **92** 2248
[30] Malyutenko V, Bolgov S and Podoltsev A 2010 *Appl. Phys. Lett.* **97** 251110
[31] Piprek J 2010 *Phys. Stat. Sol.* **207** 2217
[32] Wang L, Zhang Z and Wang N 2015 *IEEE J. Quantum Electron.* **51** 3200109
[33] Ryu H and Shim J 2011 *Opt. Express* **19** 2886
[34] Wang L, Liu Z, Guo E, Yang H, Yi X and Wang G 2013 *ACS Appl. Mater &Interfaces* **5** 5797
[35] Wang L, Zhang Y, Li X, Liu Z, Guo E, Yi X, Wang J, Zhu H and Wang G 2012 *J. Phys. D: Appl. Phys.* **45** 505102
[36] Zhu D, Xu J, Noemaun A, Kim J, Schubert E, Crawford M and Koleske D 2009 *Appl. Phys. Lett.* **94** 081113
[37] Wang L, Zhang Y, Li X, Liu Z, Zhang L, Guo E, Yi X, Zhu H and Wang G 2013 *Proc. Roy. Soc. London A: Math. Phys. Eng. Sci.* **469** 20120652
[38] Wang L, Guo E, Liu Z, Yi X and Wang G 2016 *IEEE Trans. Electron. Dev.* **63** 892